Lab on a Chip

A Novel Technique for In-situ Uniaxial Tests of Self-assembled Soft Biomaterials

Journal:	*Lab on a Chip*
Manuscript ID	LC-ART-11-2018-001273.R2
Article Type:	Paper
Date Submitted by the Author:	01-Feb-2019
Complete List of Authors:	Elhebeary, Mohamed; University of Illinois at Urbana-Champaign Department of Mechanical Science and Engineering, Emon, Md. Abul Bashar; University of Illinois at Urbana-Champaign Department of Mechanical Science and Engineering Aydin, Onur; University of Illinois at Urbana-Champaign Department of Mechanical Science and Engineering, Saif, Taher; University of Illinois at Urbana-Champaign, Mechanical Science and Engineering

A Novel Technique for In-*situ* Uniaxial Tests of Self-assembled Soft Biomaterials

Mohamed Elhebeary, Bashar Emon, Onur Aydin, and M. Taher A. Saif [*]
University of Illinois at Urbana-Champaign, Urbana, IL, USA
[*]1206 W. Green St., Urbana, IL 61801, USA E-mail: saif@illinois.edu

ABSTRACT

We introduce a novel method to form 3D biomimetic tissues from a droplet of cell-extracellular matrix (ECM) mixture on a sensor stage, and to quantify tissue force and stiffness as a function of time under optical microscopes. The method exploits advances in micro-nano fabrication and capillarity for self-assembly and self-alignment of tissues on the stage. It allows simultaneous inspection of the microstructure of the tissue *in-situ* while its mechanical response is quantified, thus linking tissue biophysics with physiology and revealing structure-function properties of 3D tissues. We demonstrate the functionality of the stage by studying mechanical behavior of different cells-collagen mixtures under mechanical, chemical and electrical stimulation. They include force evolution in cell-free collagen during curing, myotubes differentiated from muscle cell-collagen/matrigel ECM subjected to electrical stimulation, and fibroblast-collagen tissue subjected to cancer cell conditioned media (CM) and Rho-kinase inhibitor, Y27632. Muscle contraction decreases with increasing frequency of electrical stimulation, fibroblasts respond to CM by increasing contractility for a short time, and completely relax in the presence of Y27632 but restore force with Y27632 washout.

Keywords

Tissue mechanics, MEMS, muscle on-a-chip, sample self-assembly, cancer conditioned media

1. INTRODUCTION

Mechanical forces developed by cells play a critical role in the formation, maintenance, and maturation [1] of tissues. It is well established now that cells generate force using acto-myosin machinery. They also sense force and their mechanical micro-environment[2]. These forces regulate a wide range of cell functions including differentiation, receptor signaling, transcription, and proliferation. Tissues can fail to function normally if cellular processes were modulated by applying abnormal mechanical stresses [3]. Mechanical state of tissues, such as stiffness and internal forces are emerging as new prognostics for diseases as in case of liver and lung [4]. Diseased liver and pancreas regions are stiffer than their normal counterparts, as is the case of most tumors [5].

The development of multicellular tissues is highly dependent on the mechanical forces associated with cell-cell and cell-matrix interactions [6]. Despite the significance of tissue forces and mechanics in organ failures, cell-generated forces within 3D tissue environment are not well characterized. Cellular forces are commonly measured using Traction Force Microscopy (TFM) on 2D soft substrates [7], or on microfabricated arrays of micro-needle-like posts [8]. 2D studies offer simplicity, but limits cell-cell and cell-ECM interactions. 3D tissues in-*vitro* have shown the potential of mimicking some of the vital functions and behaviors of organs by recapitulating the complexity of multicellular interactions [9].

Recent studies of 3D tissues reported the influence of tissue forces to cellular gene expression [10], migration [11], wound healing [12] and morphogenesis [13]. These in-*vitro* tissues were formed by adding cells to 3D matrix of collagen and molded to the required shape, orientation and size. PDMS pillars, with known stiffness were used to constrain the tissues and measure their forces [14]. This allowed investigating the effect of different drugs on the contractile forces. Similarly, equibiaxial forces for fibroblast tissues were measured using compliant stainless steel cantilever beams [15]. By adding a nickel sphere to one of the pillars, external mechanical loading is applied to the samples using a magnetic tweezer and hence measure their stiffness [16]. Another technique for stretching microtissues is applying vacuum on PDMS cantilever beams allowing them to move apart from each other [17]. Similar effect can be achieved by stretching the substrate of the cantilevers using a motor-driven loading frame [18]. However, in all these studies, the formation of the tissue sample relies on cell-driven compaction. Hence, there is a minimum cell density needed to successfully create a tissue. Another technique utilized soft bilayer nanocomposite, composed of PDMS and graphene nanoplates, to mechanically stimulate tissues grown on its surface. The actuation is applied by exposing the cantilever beam to near infrared irradiation [19]. It was not possible to image the cells since the bilayer nanocomposite was nontransparent.

The method reported here overcomes the limitations of minimum cell density and compaction dependence of tissue formation. Here, tissues can be formed with arbitrary cell density, and tissue forces and stiffness can be measured from the early stage of formation through the entire development phase. Such in-*situ* quantitative inspection may offer new insights that cannot be achieved with existing methods. In addition, force-deformation of the tissue can be measured without exposing the tissue to any light which might affect the measured forces [20]. Small thickness of the sensor stage makes it compatible with live cell microscopy and avoid any histological sectioning needed in the case of thick samples.

2. Results and Discussions

2.1 Stage Design and Operation

Figure 1 shows the basic concept of the proposed sensor stage with biomimetic tissue (green). Here, the tissue sample, bridged between two grids, D_1D_2, is held by two springs, one hard and the other soft, with spring constants K_s and $K_h >> K_s$ respectively. The springs are held by anchors A_s and A_h. When the tissue generates a contractile force, the soft spring stretches by δ_c. Tissue force, $F(t) = K_s\,\delta_c(t)$, can be measured as a function of time using known K_s (pre-calibrated) and by optically measuring $\delta_c(t)$. In addition, the stiffness of the tissue is measured by stretching the tissue and by measuring the corresponding force to stretch. The stretch is applied by moving the anchor A_h while holding A_s fixed. This will cause the grids, D_1 and D_2, move by δ_1 (in addition to δ_c) and δ_2, respectively, giving a tissue stretch of $\delta=\delta_2-\delta_1$. Note that before stretching the tissue $\delta_1=\delta_2=0$, when $\delta_c \neq 0$, and δ_1 is the additional deformation of the soft spring due to the stretch applied to the sample. Then the total force on the tissue is $F = K_s\,(\delta_c+\delta_1)$, where $K_s\,\delta_c$ gives the active force of the tissue generated by tissue cells, and tissue stiffness, $K_{tissue}= dF/d\delta$, where δ_1, δ_2, and δ_c are measured optically.

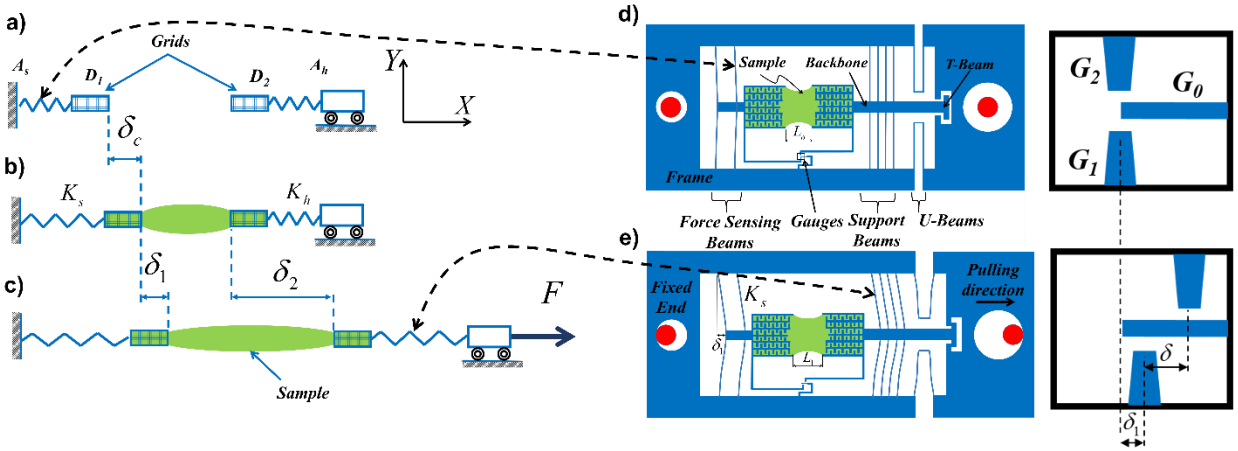

Figure 1 a) Conceptual design of the stage with two grids and springs, b) sample is formed by dispensing sample material between two grids and generates contractile force, F(t) = Ks δc(t),(c) The stiffness of the tissue is measured by stretching, schematic of the stage with the sample (green) forming a bridge with the corresponding gauges positions (on the right) d) before, and e) during stretching

The concept of Figure 1-a is implemented in the design shown in Figure 1d. It consists of a rigid frame, backbone, two grids, two U-beams, force sensing beams, support beams, and displacement measurement gauges, G_0, G_1 and G_2. A sample (green) is formed between the grids with length L_o. There is a hole at each side of the frame. Rigid pins (red circles in Figure 1d), through the holes, are used to stretch the stage and apply tensile loading on the sample. Upon loading, the T-beam latches and the support beams transfer the load to the sample (Figure 1e). The function of the U-beams of the stage (Figure 1d) is to suppress any misalignment between the direction of stretching of the stage and the specimen longitudinal axis by six orders of magnitude [21]. Since the sample and the force sensing beams are in series, the load on the sample is transferred to the force sensing beams with stiffness K_s, and can be obtained from their deformation. The stiffness, K_s, of the force sensing beams can be calibrated using AFM or nanoindentation. It can be estimated by $K_s = 12nEI/L^3$ where n, E, L, and I are the number of beams, elastic modulus of silicon (*169 GPa* along <110> direction), length of beams, and second moment of inertia

($I=1/12bh^3$ where b and h are the beams' width and depth), respectively. The dimensions of the beams are measured at high resolution using SEM. The force F deforms the force sensing beams by $\delta_1=L_1-L_0$ giving a measure of the force $F=K_s\,\delta_1$ (Figure 1d).

Gauges G_0, G_1 and G_2 are used to measure the force and deformation in the sample (Figure 1d), located at a proximity from the sample (approx. *1 mm*) to reduce the sample exposure to light during the experiment. G_0 is the reference gauge attached to the stationary rigid frame, G_1 is attached to the grid on the force sensing beams side, and G_2 is attached to the grid on the supporting beams side. Upon loading the change in the gap (δ_1) between G_0 and G_1 is measured and used to calculate the applied force on the sample F. The change in gap between G_1 and G_2 gives the total deformation (δ) of the sample and hence strain is calculated as $\varepsilon=\delta/L_o$.

The above design is micro-fabricated from a double side polished *100 mm* diameter, *200 μm* thick silicon wafer, with (1 0 0) orientation. First, one side is patterned using photolithography. A positive photoresist (SPR 220 4.5) is spun coat, and exposed to UV light under a contact mask aligner with a dose of 160 mJ/cm^2 (Electronic Visions EV620, i-line). To obtain vertical sidewalls for all the beams, deep reactive ion etching (DRIE) of silicon is used (STS Pegasus ICP-DRIE). The photoresist is then removed by reactive ion etching (RIE) process using oxygen and argon plasma. A protecting beam (*10 μm*) guards the soft force sensing beams during fabrication shown in Figure 2a. Before the experiment, the protecting beam is removed using a fine needle. SEM image of a micro-fabricated stage is shown in Figure 2a, where the supporting beams' dimensions are approximately: *L = 6 mm, b = 200 μm, h = 20 μm.* The force sensing beams have the same length and width but smaller thickness, designed between *5* to *15 μm*. Correspondingly, the stiffness of force sensing beams (K_s) ranges between *0.625* to *25.35 μN/μm.* Gauges are approximately *15 μm* apart, and located at a close proximity to the sample (Figure 2b). A zoom-in-view of the grids with a *500 μm* gap between them to form the sample is shown in Figure 2c.

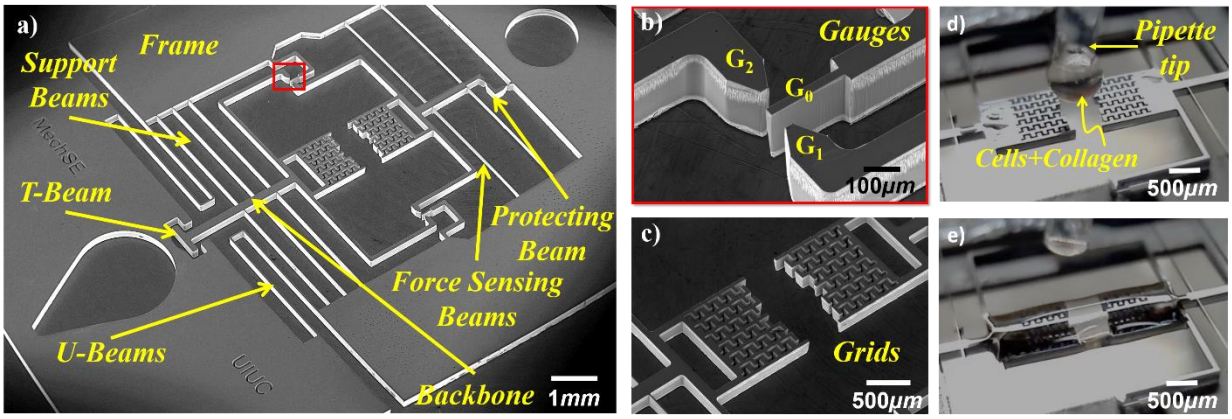

Figure 2 a) SEM image of the stage with b) zoom-in view of the sensor gauges and c) specimen. The gripping mechanism of the stage during d) forming the droplet on the tip of the pipette and e) after filling the channels and sample formation

A syringe pump (NE-1000; New Era, Farmingdale, NY) is used to drive the sample's material through flexible tube to a fine needle with controlled volume and flow rate. The needle is fixed to a 3D automated stage equipped with piezoactuators with fine steps (few nms) to precisely dispense cell-ECM (collagen and/or matrigel in this paper) liquid mixture in the space between the two grids (see Figure 2d-e, supplementary movie S1). All the components are kept at 0ºC before dispensing to avoid early polymerization of ECM. The sensor stage is mounted on a spacer near

the base to avoid any contact of the dispensed liquid with the substrate. To stretch the sample, the stage is held fixed at one end using a rigid pin that goes through the hole in the chip, while deformation (along the axial direction of the sample) is applied at the other end by a piezo-actuator using a second rigid pin. Strain rates can be varied from $1*10^{-4}$ to $3*10^{-3}$ s^{-1}.

Testing and imaging are carried out using an inverted optical microscope (Olympus IX81, 40× lens, Olympus America Inc., Center Valley, PA) mounted on a vibration isolation table (Newport Corporation, Irvine, CA). The microscope stage is enclosed by an environmental chamber that maintains cell culture conditions throughout imaging (5% CO_2, 70% humidity and 37° C). Images are acquired with a Neo sCMOS camera (active pixels 1392 × 1040, resolution of 167 nm per pixel) (Andor Technology, Belfast, Northern Ireland). Images are taken for the sensor gauges to calculate displacements using template matching plugin in imageJ with subpixel resolution [22,23]. Image analysis gives a displacement resolution of approximately *17 nm*. This gives a force resolution of approximately *11 nN* (K_s*=0.625 µN/µm).* The stage allows us to measure force of the biomimetic tissue as a function of time without "seeing" the tissue. This saves the tissue from light exposure which may result in light induced tissue response [20]. However, the tissue can be imaged by programming the microscope stage to step between the tissue and the gauge locations precisely. Note that the force measurement resolution depends on the force sensing beams' stiffness, which depends on their dimensions. Hence the stiffness can be widely varied by changing geometry of force sensing beams (FSB). Here, all FSBs were 6 mm in length and the smallest thickness we were able to fabricate was 5 µm, resulting in a stiffness, K_s*=0.625 µN/µm,* and force resolution of 11 nN.

Note that the sensor stage is made from single crystal silicon. Silicon forms a thin layer of native oxide which makes its surface hydrophilic. Thus, the grid with a network of open channels draws the cell-ECM mixture (aquous based) into the channels due to capillarity, and no external effort is required to drive the sample into the final shape. Thus, the tissue construct undergoes a self-assembly process regardless of cell density. This technique can be used for all soft materials that can be dispensed in a liquid form before polymerization (Figure 2d). The ECM cures in few minutes when the sample gets gripped and anchored by the channels (Figure 2e). The stage with the bridge is then inundated in cell culture media.

2.2 Collagen Characterization

A droplet of liquid collagen type-1 (Corning), from rat tail tendon, is dispensed on the grids to form the bridged sample (Figure 2d-e). It is left for 15-20 mins to polymerize in a humidified environment at room temperature. Following polymerization of the collagen, the stage is submerged in Phosphate buffered saline (PBS) and clamped to the petri dish floor. The petri dish is clamped to the microscope stage inside the environmental chamber for time lapse imaging of the gauges and sample.

Low concentration collagen matrices are usually used in tissue engineering studies in-vitro. Hence, their mechanical characterization is crucial for understanding the overall tissue response. Here, collagen samples with 2mg/mL concentration were first tested by the sensor stage. The gauges showed an initial force of 12.7 µN, soon after the collagen sample was inundated in PBS. The displacement of the gauges was monitored for the next 10 hours, and showed a gradual drop in the load (Figure 3a). The load stabilizes after approximately 6 hours at 84% from the original value. The relaxation might be due to absorption of water and corresponding swelling of collagen sample, as well as unbinding of weak bonds [24].

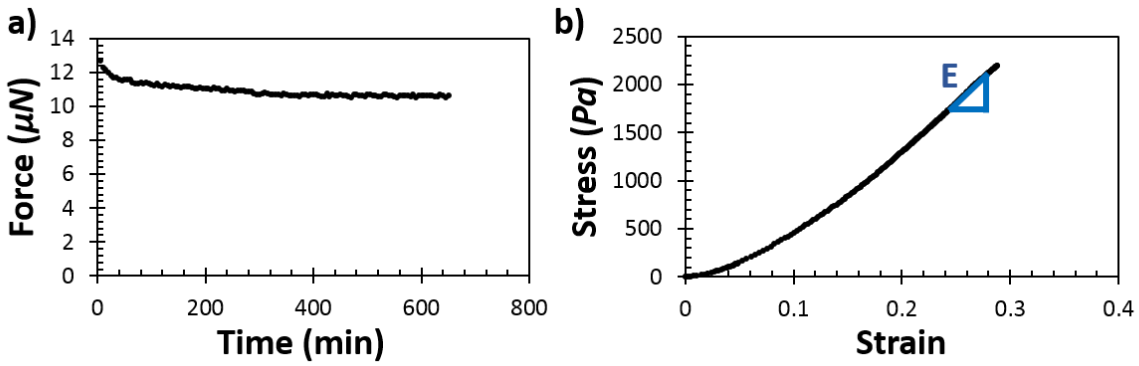

Figure 3 a)Force measurement after sample formation and b)Stress-strain relationship for collagen sample (2 mg/mL)

The dimension of the collagen samples at mid-section were measured from the optical images. Different strain rates were applied to different samples. Engineering stress and strain are calculated from the load displacement data. Engineering stress is calculated as $\sigma=F/A$, where F is the force transmitted through the sample given by $F=K_s \delta_1$ (Figure 1), where A is the cross sectional area of the sample. Engineering strain is calculated as the change in length (ΔL) divided by the original length between the grids (L_o), and is given as $\varepsilon=\Delta L/ L_o$. Upon stretching, all samples exhibited a similar stress-strain relationship (supplementary movie S2). It starts with a nonlinear region followed by a linear one that is used to calculate the elastic modulus, given as $E=\Delta\sigma/\Delta\varepsilon$ (Figure 3b). The elastic moduli were *6.7* and *8.3 KPa* for samples with concentrations *1* and *2 mg/mL*, respectively at a strain rate of approximately $8*10^{-4}$ s^{-1}. At a higher strain rate ($3*10^{-3}$ s^{-1}) collagen sample at *2 mg/mL*, showed an increase in the elastic modulus of 9.5 KPa.

2.3 Fibroblast Tissues

Here, 3T3 cells are mixed with collagen (*2 mg/mL*) before dispensing the liquid mixture on the grids (approx. cell density=5 *million/mL*). Within few hours, the collagen matrix is contracted by cells (Figure 4). Single cell activity can be monitored during this process and it shows how the cells move towards the center, pulling the edges (see supplementary movie S3). Figure 5a shows the force evolution within the tissue for 100 hrs after dispense. There is an initial jump in force due to collagen force alone. The force then drops by a small percentage of the initial force, possibly due to swelling of collagen mixture (see Figure 3 for collagen only sample). The cell-collagen tissue then increases force after 3 hrs. This force is due to fibroblast adhering to collagen and becoming contractile, thus compacting the tissue. The rate of increase of force with time decreases in about 5 hrs after which the rate becomes constant. During the first 300 mins, the radius of curvature of the sample increases, after which it remains constant (Figure 5c). After 100 hrs the tissue force reached to *51 μN*, i.e., the force contributed by the cells is about *20 μN* with estimated collagen force of about *30 μN*.

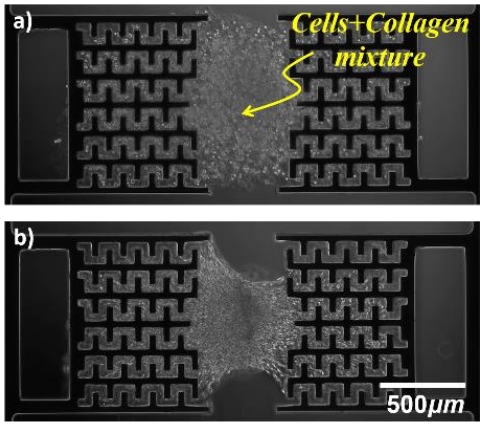

Figure 4 Cells/collagen mixture (approx. cell density=5 milion/mL*) a) right after dispensing onto the stage and d) after 24 hours of contraction*

To test whether the force is due to fibroblast contractility, we apply Y27632 (Rho-kinase inhibitor to disrupt non-muscle myosin II (20 μM)) and relax fibroblast force (Figure 5b) at 100th hr. The force drops exponentially to nearly a steady value of *34.5 μN* in *20 mins*. The small scale of our microtissue allowed fast diffusion of Y27632 within few seconds. Then we washed out Y27632 with fresh media and left in the incubator for *60 mins* without time lapse imaging. After *60 mins*, the force was recorded as *46 μN*, validating that the tissue force was indeed actively maintained by 3T3 cells. This force reversibility, i.e., relaxation of force to initial value (*30 μN*) and its restoration to pre-relaxation state suggest that fibroblasts did not significantly remodel the matrix during 100 hrs. The cells only contracted the gel elastically. Hence, when most of the cell force was relaxed with Y27632, the tissue was un-deformed to initial configuration. The process was reversible with washout of Y27632.

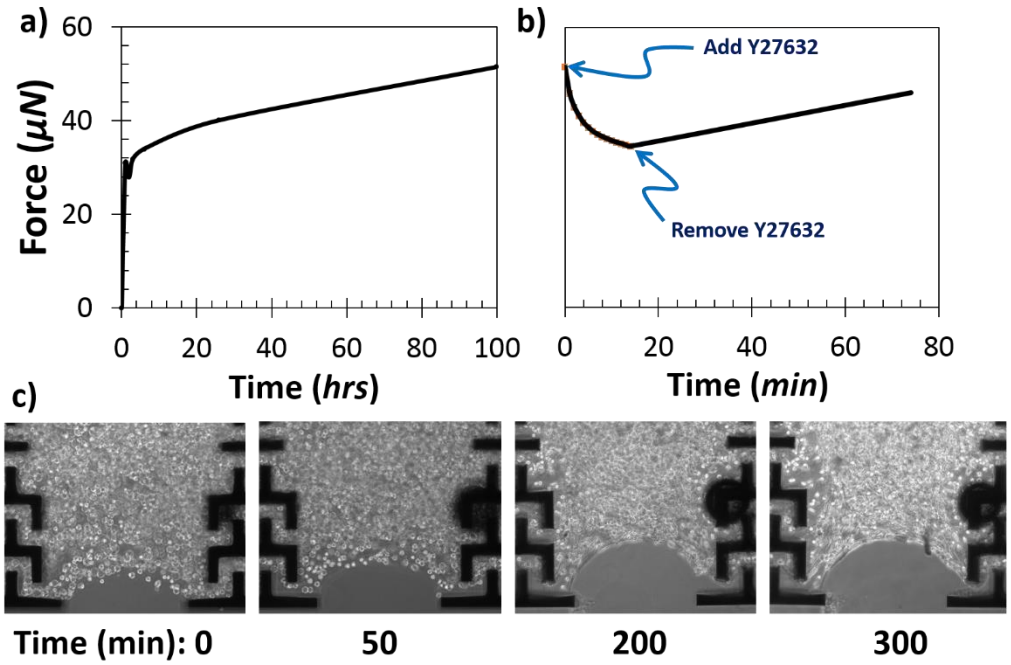

Figure 5 Force vs time of tissue during a) formation (with a collagen sample, b) addition/removal of Y27632 (Rho-kinase inhibition) and c) different stages during compaction of tissue with time

We then stretched the sample to measure its force response and its stiffness. From the cross-sectional geometry of the sample (measured by confocal microscope after force-stretch test), we evaluated the corresponding stress-strain response (Figure 6a) which shows a nonlinear behavior. The elastic modulus is about *4 KPa* at small strain, but *13 KPa* at 10% strain. The high modulus at small strain is possibly due to the large tensile strain of the collagen induced by the contractile cells. The tissue was inspected in multimodal multiphoton microscope with label-free second harmonic generation imaging technique [25] or SHG mode to visualize collagen network, and cells by fluorescing actin using SiR-Actin (Cytoskeleton, Inc). The cell (red) shows filopodial protrusion, possibly stretching the collagen matrix (Figure 6b).

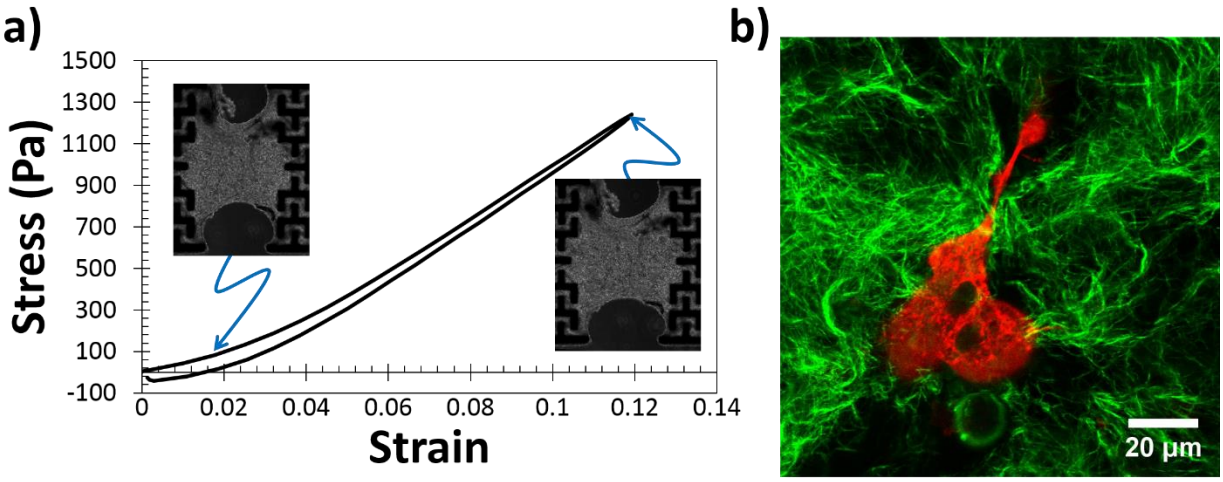

Figure 6 a) Stress-strain relation of cell/collagen (approx. cell density=5 million/mL) and b) confocal microscopy image of collagen (green) using SHG and cell actin (red) using SiR-Actin

2.4 Muscle on-the-chip

Next, we used skeletal muscle cells to demonstrate the ability of our stage to measure force dynamics in much shorter time scales compared to the quasi-static fibroblast contractility. Tissues were formed by embedding C2C12 mouse skeletal myoblasts in an ECM gel consisting of type I collagen and Matrigel, following the same procedure for fibroblast-laden tissues. After formation, tissues (Figure 7a) were cultured in muscle differentiation medium to allow myogenic differentiation. C2C12 cells embedded in ECM gels retain their ability to differentiate into myotubes [26] which can generate contractions in response to electrical stimulation [27,28]. Indeed, after three weeks of incubation in muscle differentiation medium, the C2C12 tissues on our platform produced muscle contractions in response to electrical stimulation (Figure 7b, Movie 1). Tissues were stimulated using a custom setup. Two platinum wire electrodes were placed 15mm apart with the sample located in the middle. A DC power supply and an Arduino board were used to deliver 0-9V (0-6V/cm) with 5ms pulse width at frequencies ranging from 1 to 20Hz. Here, we stimulated the muscle tissues using a uniform electric field which excites all myotubes simultaneously, resulting in a uniform contraction of the whole tissue (supplementary movie S4).

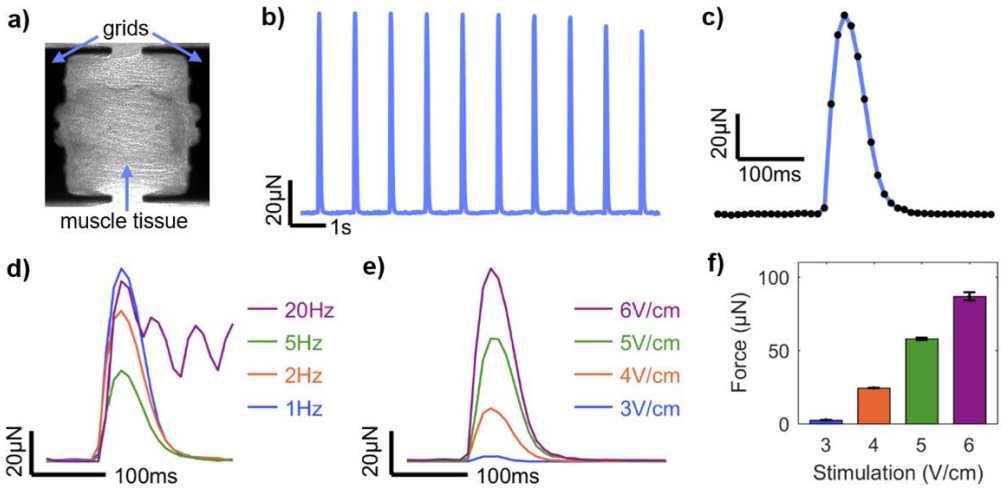

Figure 7(a) Brightfield image of a muscle tissue sample after 3 weeks in culture. (b) Muscle contraction forces induced by electrical stimulation at 1Hz and 6V/cm, recorded for 10s. (c) Force-time curve of a representative muscle contraction. Black dots are actual data points. (d) Time profiles of individual contractions from different stimulation frequencies. (e) Force-time curves of contractions corresponding to different electric field strengths. (f) Peak contraction force vs. stimulation magnitude. Values are mean ±SD, n=10 contractions for each condition.

Using high speed imaging (100 fps), we were able to quantify force profile during a single muscle contraction. Upon stimulation by an electrical pulse, muscle begins to contract, and force rises for approximately 30ms. After reaching peak contraction, the muscle tissue relaxes for approximately 100ms with the force returning to the rest value (Figure 7c). When stimulated at 1, 2, or 5Hz, each individual contraction follows the same time-profile with different amplitudes (Figure 7d). However, when stimulated at 20Hz, corresponding to 50ms gap between the start of two consecutive voltage pulses, the tissue is not given enough time to relax fully to the rest state before the next contraction begins. This results in what is known as summation, where the muscle remains partially contracted during the stimulation period (Figure 7d). The muscle contractions also follow the same time-profile when stimulated at different electric field strength (Figure 7e). In this study, we used stimulation with field strength ranging from 3V/cm to 6V/cm. Within this range, the peak value of muscle contraction force increases linearly with stimulation magnitude (Figure 7f).

2.5 Fibroblast Tissue Construct under Cancer Conditioned Media

Human colon fibroblast cells, CCD18co, was used to form a fibroblast tissue construct with collagen I (2 mg/ml). Cell density was approximately 1 million/ml. After a polymerization period of about 20 minutes, the stage was submerged in culture media. The tissue construct and the force sensor were monitored for 24 hours for the tissue construct force to stabilize. After initial 24 hours, the culture media was replaced by cancer conditioned media which was prepared from the serum-free culture media of FET colon cancer cell for 72 hours and supplemental FBS (detailed description in CELL CULTURE AND REAGENTS section). The conditioned media is enriched with the growth factors released by cancer cells, e.g. Transforming growth factor β (TGFβ1-3), Interleukin-6 (IL-6), Interleukin-13 (IL-13), Colony stimulating factor 1 (CSF-1), Vascular endothelial growth factor (VEGF) etc.[29–31]. These growth factors, especially TGFβ, are known to induce differentiation of stromal fibroblast into myofibroblast or cancer associated fibroblast (CAF) [32]. After approximately 48 hours of culture in conditioned media, tissue costruct force was relaxed using 10 μM solution of ROCK inhibitor Y-27632 for 15 minutes in order to investigate

permanent deformation and remodeling of the tissue construct by fibroblast activity. The drug was then washed out to allow the cells to regenerate the tissue construct tension. Force activity was monitored for 24 subsequent hours (Figure 8).

Tissue construct forces build up during first 10-20 hours after formation. After this period, the tissue construct usually maintains this force if the cell density is high. For low density tissue constructs, tension fluctuates with time and sometimes can drop significantly. In our samples we observed a gradual reduction in forces during 12 to 24 hours of culture. During this period, we noticed cell division and movement which we assume resulted in a force relaxation by about 20%. At this point, cancer condition media was introduced in the culture condition and was maintained for subsequent 48 hour. Cancer cell derived growth factors in the conditioned media evidently brought about an increase in tissue construct force in all the samples. Increment in force varied from 15% to 60%. This result suggests that fibroblasts are responding to growth factors from cancer cells in a three-dimensional culture condition which corroborates results from 2D culture traction force microscopy that reported traction force increase with growth factor stimulation [33,34]. Moreover, tissue construct images show that the cells after conditioned media treatment (48^{th} hour) are appreciably more elongated and phenotypically tense compared to the cells (20^{th} hour) before cancer media application (Figure 8). Interestingly in some samples, the effect of conditioned media was transient, and the tissue construct force stabilized at the peak value observed before addition of cancer media. This can be an indication that the fibroblasts need a continuous supply of stimulating media to maintain a heightened tensile state; but it has to be confirmed through more experiments.

After treatment with Y-27632, tissue construct force drops to zero within about 20 mins. After washout, tissue construct force returned to the pre CM (not post CM) level within about 2 hours. This suggests that the cells have no memory of the CM they were exposed to and they need the growth factors from CM to maintain high force level.

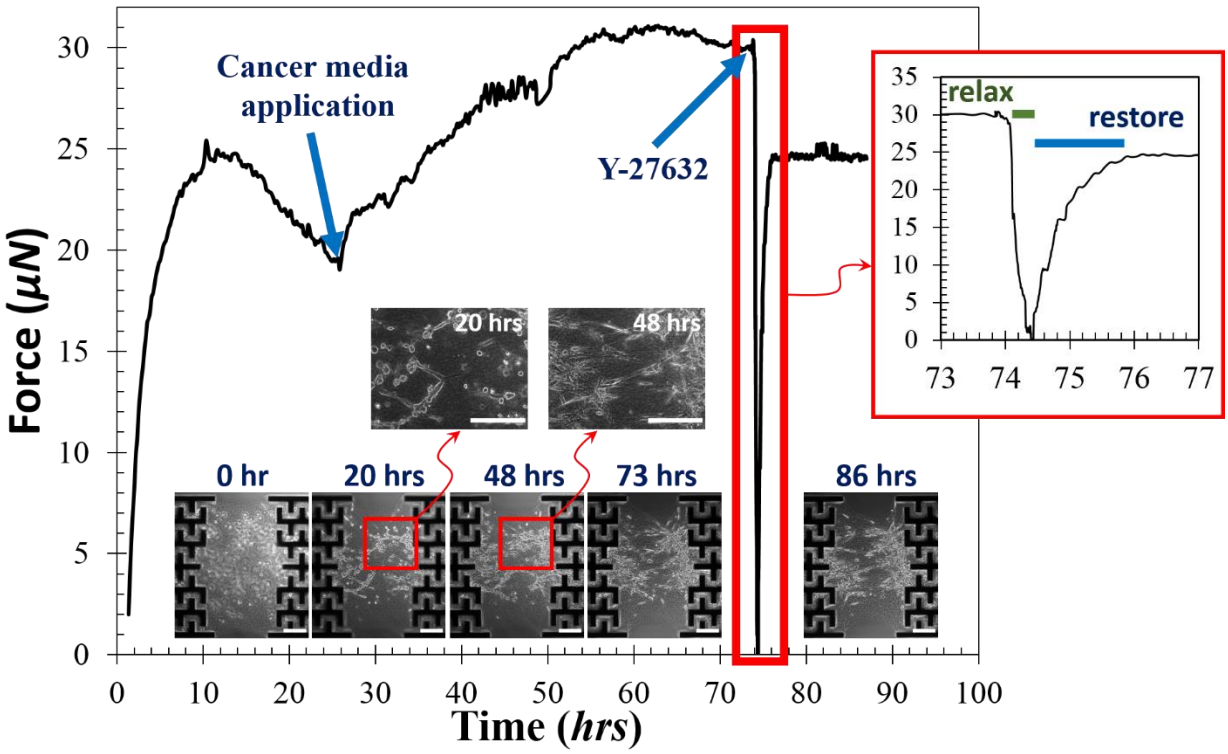

Figure 8 Cancer conditioned media and drug influence the tissue construct force on the device. Force evolution with time for CCD18co fibroblast tissue construct after formation. Brightfield images of the tissue construct at different time points show how the cells adhere to ECM, spread and build up tension in the tissue construct. Zoomed in images at 20 and 48 hrs demonstrate that the same cells exhibit a more elongated and tense phenotype after treatment with cancer media. Treatment with Y-27632 drug results in a sharp decline in tissue construct force within 20 mins, but after washout, it took about 2 hrs to restore the force. Scale bars 200μm.

3. Conclusions

We present a novel platform that allows studying the mechanical behavior of freestanding biomaterial samples. Both collagen and tissue constructs were tested in controlled environment under optical microscope. Samples were exposed to mechanical, chemical and electrical stimulation. We introduce, for the first time, a self-assembly technique for samples using capillary action. Hence, this unique feature allows any mixture of ECM and cells to be tested regardless of their initial density and self-compaction ability.

4. Experimental Section

For all tissue seeding procedures, ECM solution was prepared on ice by first neutralizing type I collagen from rat tail (Corning) with 1N sodium hydroxide, 10X phosphate buffered saline, and molecular biology grade water. For C2C12 tissues, neutralized collagen is mixed thoroughly with growth factor reduced Matrigel (Corning). Collagen and Matrigel were used at final concentrations of 2mg/ml each. C2C12 cells were suspended in ECM solution at a density of 2.5×10^6 cells/ml. Cell-ECM mixture was then seeded onto the device and was allowed to polymerize at room temperature for 30min. Samples were then inundated in growth medium. After 2 days, culture medium was switched to muscle differentiation medium. Samples were kept in muscle differentiation medium with daily medium replacements until termination of the experiments.

4.1. Cell Culture and Reagents

Collagen type-1 (Corning) from rat tail tendon with initial concentration 8.9 mg/mL was used. For each experiment 1 mL of collagen was prepared at a final concentration 2mg/mL and pH 7.4 by mixing 100 uL of 10X Phosphate buffered saline (PBS), 224.7 µL of collagen (conc. 8.9 mg/mL), 670.1 µL dH2O, and 5.2 µL 1N NaOH. For tissue samples, NIH 3t3 cells were mixed with collagen type-1 gels before seeding on the device. NIH 3T3 cells obtained from ATCC were cultured in high glucose DMEM containing 10% fetal bovine serum, 2 mM L-glutamine, 100 units/mL penicillin, and 100 mg/mL streptomycin (all from Invitrogen)

C2C12 skeletal myoblasts (ATCC) were maintained below 70% confluency in growth medium consisting of high-glucose Dulbecco's modified Eagle's medium (DMEM), 10% v/v fetal bovine serum (FBS), and 2mM L-Glutamine. To facilitate myotube formation, tissues were cultured in muscle differentiation medium consisting of high-glucose DMEM, 10% v/v horse serum, and 2mM L-Glutamine (all reagents from Gibco). All C2C12 cells were used at passage number 5.

CCD18co colon fibroblasts and FET colorectal carcinoma cells were a gift from the lab of Prof. Barbara Jung, Dept. of Medicine, UIC. Fibroblast culture media was prepared using 90% Dulbecco's Modified Eagles Media (DMEM, Corning) and 10% Fetal Bovine Serum (FBS, Gibco). FET cells were maintained in 89% Dulbecco's Modified Eagles medium/F12 50:50 (Gibco), 10% Fetal Bovine Serum (FBS, Gibco) and 1% Penicillin-Streptomycin (Lonza). For cancer conditioned media, FET colon cancer cells were cultured in a serum free media for 72 hours and then this media was harvested, mixed with DMEM at 1:1 ratio and supplemented with 10% FBS. Collagen used for tissue preparation was rat-tail collagen I (Corning). Y-27632 (Sigma-Aldrich) was used as ROCK-inhibitor.

4.2. Staining

SiR-Actin from Cytoskeleton,Inc was used for labelling F-actin in live cells in the formed tissue. SiR-Actin was diluted to 100 nM with media, and left in the incubator at 37 C in a humidified atmosphere containing 5% CO2 for 12 hours before imaging. A standard Cy5 filterset was used during confocal imaging. Second harmonic generation (SHG) imaging was used to image collagen fibers. Zeiss LSM 710 confocal microscope equipped with Mai-Tai Ti-Sapphire laser was used. The excitation wavelength was 780 nm.

Contributions

ME and *TS* conceived the idea and designed experiments, *ME*, *BE* and *OA* conducted experiments and analyzed data, and all authors wrote the manuscript.

Conflicts of interest

There are no conflicts to declare

Acknowledgements

This project was funded by the National Science Foundation (NSF) award No.1562694. It was also partially supported by the National Institute of Biomedical Imaging and Bioengineering of the National Institutes of Health under Award Number T32EB019944. The content is solely the responsibility of the authors and does not necessarily represent the official views of the National

Institutes of Health. The single crystal silicon stages were fabricated in Micro-Nano-Mechanical Systems Laboratory at University of Illinois Urbana Champaign (UIUC). Scanning electron microscope imaging was performed in the Microscopy Suite at Beckman Institute for Advanced Science and Technology at UIUC. Confocal imaging was carried out at the institute for genomic biology at UIUC.

REFERENCES

1 M. KJAeR, *Physiol. Rev.*, 2004, **84**, 649–698.

2 D. E. Discher, P. Janmey and Y.-L. Wang, *Science*, 2005, **310**, 1139–43.

3 D. E. Jaalouk and J. Lammerding, *Nat. Rev. Mol. Cell Biol.*, 2009, 10, 63–73.

4 H. R. Wirtz and L. G. Dobbs, *Respir. Physiol.*, 2000, **119**, 1–17.

5 W.-C. Yeh, P.-C. Li, Y.-M. Jeng, H.-C. Hsu, P.-L. Kuo, M.-L. Li, P.-M. Yang and P. H. Lee, *Ultrasound Med. Biol.*, 2002, **28**, 467–474.

6 P. Ekblom, D. Vestweber and R. Kemler, *Annu. Rev. Cell Biol.*, 1986, **2**, 27–47.

7 M. Dembo and Y.-L. Wang, *Biophys. J.*, 1999, **76**, 2307–2316.

8 J. L. Tan, J. Tien, D. M. Pirone, D. S. Gray, K. Bhadriraju and C. S. Chen, *Proc. Natl. Acad. Sci.*, 2003, **100**, 1484–1489.

9 K. L. Schmeichel, *J. Cell Sci.*, 2003, **116**, 2377–2388.

10 A. S. Piotrowski-Daspit, J. Tien and C. M. Nelson, *Integr. Biol.*, 2016, **8**, 319–331.

11 N. Gjorevski, A. S. Piotrowski, V. D. Varner and C. M. Nelson, *Sci. Rep.*, 2015, **5**, 11458.

12 M. S. Sakar, J. Eyckmans, R. Pieters, D. Eberli, B. J. Nelson and C. S. Chen, *Nat. Commun.*, 2016, **7**, 11036.

13 N. Gjorevski and C. M. Nelson, *Integr. Biol.*, 2010, **2**, 424.

14 W. R. Legant, A. Pathak, M. T. Yang, V. S. Deshpande, R. M. McMeeking and C. S. Chen, *Proc. Natl. Acad. Sci.*, 2009, **106**, 10097–10102.

15 J. John, A. Throm Quinlan, C. Silvestri and K. Billiar, in *Annals of Biomedical Engineering*, 2010, vol. 38, pp. 658–673.

16 R. Zhao, T. Boudou, W. G. Wang, C. S. Chen and D. H. Reich, *Adv. Mater.*, 2013, **25**, 1699–1705.

17 M. Walker, M. Godin and A. E. Pelling, *Biomed. Microdevices*, 2018, **20**, 43.

18 M. Asmani, S. Velumani, Y. Li, N. Wawrzyniak, I. Hsia, Z. Chen, B. Hinz and R. Zhao, *Nat. Commun.*, , DOI:10.1038/s41467-018-04336-z.

19 W. Jiang, D. Niu, L. Wei, G. Ye, L. Wang, H. Liu, P. Chen, F. Luo and B. Lu, *Carbon N. Y.*, 2018, **139**, 1048–1056.

20 S. G. Knoll and M. T. A. Saif, *Extrem. Mech. Lett.*, 2016, **8**, 257–265.

21 M. Haque and M. Saif, *Exp. Mech.*, 2002, **42**, 123–128.

22 C. A. Schneider, W. S. Rasband and K. W. Eliceiri, *Nat. Methods*, 2012, **9**, 671–675.

23 Q. Tseng, I. Wang, E. Duchemin-Pelletier, A. Azioune, N. Carpi, J. Gao, O. Filhol, M. Piel, M. Théry and M. Balland, *Lab Chip*, 2011, **11**, 2231.

24 S. Nam, K. H. Hu, M. J. Butte and O. Chaudhuri, *Proc. Natl. Acad. Sci.*, 2016, **113**, 5492–5497.

25 M. Sivaguru, S. Durgam, R. Ambekar, D. Luedtke, G. Fried, A. Stewart and K. C. Toussaint, *Opt. Express*, 2010, **18**, 24983.

26 C. Rhim, D. A. Lowell, M. C. Reedy, D. H. Slentz, S. J. Zhang, W. E. Kraus and G. A. Truskey, *Muscle Nerve*, 2007, **36**, 71–80.

27 M. S. Sakar, D. Neal, T. Boudou, M. A. Borochin, Y. Li, R. Weiss, R. D. Kamm, C. S. Chen and H. H. Asada, *Lab Chip*, 2012, **12**, 4976.

28 D. Neal, M. S. Sakar, R. Bashir, V. Chan and H. H. Asada, *Tissue Eng. Part A*, 2015, **21**, 1848–1858.

29 B. Emon, J. Bauer, Y. Jain, B. Jung and T. Saif, *Comput. Struct. Biotechnol. J.*, , DOI:10.1016/J.CSBJ.2018.07.003.

30 C. Bellomo, L. Caja and A. Moustakas, *Br. J. Cancer*, 2016, **115**, 761–769.

31 E. Witsch, M. Sela and Y. Yarden, *Physiology*, 2010, **25**, 85–101.

32 H. Chen, W.-W. Yang, Q.-T. Wen, L. Xu and M. Chen, *Exp. Mol. Pathol.*, 2009, **87**, 189–194.

33 G. S. Karagiannis, T. Poutahidis, S. E. Erdman, R. Kirsch, R. H. Riddell and E. P. Diamandis, *Mol. Cancer Res.*, 2012, **10**, 1403–1418.

34 B. Erdogan, M. Ao, L. M. White, A. L. Means, B. M. Brewer, L. Yang, M. K. Washington, C. Shi, O. E. Franco, A. M. Weaver, S. W. Hayward, D. Li and D. J. Webb, *J. Cell Biol.*, 2017, **216**, 3799–3816.

A novel method for the characterization of soft bio-materials and 3D tissues with living cells. Samples are self-assembled from a liquid droplet of the biomaterial on the testing stage.